Thermal Isomerization of 12-Oxa-1,9-dimetylhexacyclo[7.2.1.$0^{2,4}$.$0^{2,8}$.$0^{3,7}$.$0^{6,8}$]-dodec-10-ene: A Computational Mechanistic Investigation

by **Susanne Glück-Walther**[1]), and **Günter Szeimies***[2])

Institut für Chemie, Humboldt-Universität zu Berlin, Brook-Taylor-Straße 2, D-12489 Berlin
(e-mail: drszeimies@aol.com)

Dedicated to Professor *Rolf Huisgen* on the occasion of his 85th birthday

Flash-vacuum pyrolysis of the quadricyclane derivative **5a** at 350° afforded the oxabishomocubane **9a**, whose structure was confirmed by an INADEQUATE-NMR experiment. A computational investigation of the mechanism of this unexpected reaction by DFT and CASPT2-SCF methods indicated that the reaction path of lowest energy involves a quadricyclane/oxaquadricyclane (**5**/**12**) isomerization, followed by a well-established cycloreversion of **12** to the carbonyl ylide **16**, which subsequently undergoes an intramolecular 1,3-dipolar cycloadditon to **9**. The lowest-energy path of the thermal isomerization of the *syn*-quadricyclane **6c** is its conversion to the *syn*-sesquinorbornatriene **8c**. The corresponding *anti*-isomer **5c**, however, shows the capability of a degenerate quadricyclane/quadricyclane rearrangement.

1. Introduction. – Some time ago, we showed that the quadricyclane (=tetracyclo[3.2.0.$0^{2,7}$.$0^{4,6}$]heptane) derivatives **1**, **2**, and **3** can be generated as reactive intermediates in solution by metal halide elimination of appropriately substituted precursors, and could be trapped as *Diels–Alder* adducts by organolithium compounds or by cyclic 1,3-dienes [1–3]. Despite considerable experimental effort, we were unable to provide evidence for the existence of the remaining 2,3-dehydroquadricyclane **4** [4][5], which, according to computational results, is the least-stable isomer within this series of compounds [3][6].

The *Diels–Alder* trapping products of **1**–**3** appeared interesting because they open access to norbornadiene derivatives that are not easily available by alternative synthetic routes. This seemed especially true for the products of the reaction of 2,5-dimethylfuran with **2**, which afforded a 3:1 mixture of the *anti*- and *syn*-adducts **5a** and **6a**, respectively [2]. Thermal isomerization of **5a**/**6a** was expected to lead to the oxasesquinorbornatrienes **7a** and **8a**. Their hydrocarbon counterparts **7c** and **8c**, respectively, have been the subject of intensive investigation by *Paquette* and co-workers [7–9]. Recently, *Camps* and co-workers found that a *syn*-sesquinorbornatriene derivative showed enhanced reactivity of the tetrasubstituted C=C bond [10], which could also be expected for **7a**/**8a**.

---

[1]) Work carried out at the Institut für Organische Chemie, Universität München.

[2]) Correspondence address: Pfingstrosenstrasse 41, D-81377 München.

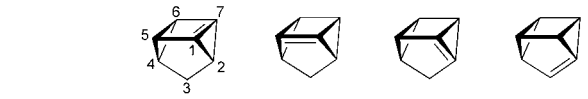

1 **2** **3** **4**

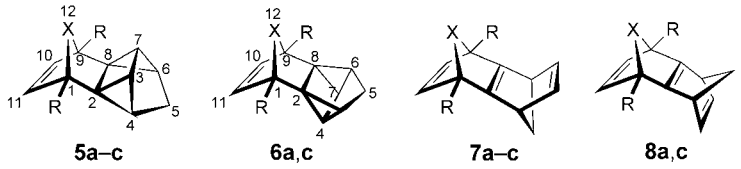

5a–c **6a,c** **7a–c** **8a,c**

a X = O, R = Me
b X = O, R = H
c X = CH_2, R = H

2. Results and Discussion. – 2.1. *Experimental Results.* An approximately 3:1 mixture of **5a**/**6a** was subjected to a flash-vacuum-pyrolysis procedure at 350° (oven temperature) at 0.001 Torr. The volatile products were collected in a trap cooled with dry-ice/acetone. The recovery of the material amounted to 83%. After removal of some polymeric material, NMR analysis showed that no starting material was present and that 2,4-dimethyl-3-oxahexacyclo[5.5.0.$0^{1,10}$.$0^{2,6}$.$0^{4,10}$.$0^{5,9}$]dodec-11-ene (**9a**) had been formed as the sole product.

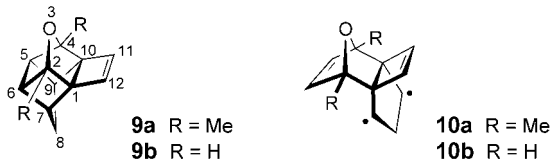

9a R = Me
9b R = H

10a R = Me
10b R = H

The structure of **9a** was established by NMR spectroscopy, the signals indicating a plane of symmetry. Of specific help was an INADEQUATE experiment [11], which furnished the connectivity of the carbon framework *via* $^{13}C,^{13}C$ coupling constants (*Table 1*). In addition, the $^{13}C,^{13}C$ coupling constants were calculated with Gaussian 03 [12] at the B3PW91/6-311G**//B3PW91/6-311G** level of theory. Although the calculated ^{1}J(C,C) coupling constants are systematically smaller than the experimental values, the structural relations are well reflected in the calculated values.

The outcome of the thermal isomerization of **5a** was unexpected. Looking at the structure of **5a**, an obvious route to product **9a** would be the breaking of the C(3)–C(4) and C(6)–C(7) bonds, which would lead to the formation of the biradical **10a**, which, in turn, could add to the remote C=C bond to give **9a**. At this point, it seemed necessary to look somewhat closer to the energy of the corresponding hypersurface by computational methods.

2.2. *Computational Investigation of the Thermal Rearrangement of* **5b**. 2.2.1. *Methods.* The thermal isomerization of the simpler model compound **5b** was studied with the aid of density functional theory (DFT), using the three-parameter functional of *Becke* [13], and the correlation functional of *Perdue* and *Wang* [14]. The unrestricted

Table 1. *$^{13}C,^{13}C$-NMR Coupling Constants of* **9a**

Coupling constant	Experimental	Calculated[a])
^{1}J [Hz]:		
C(1)–C(2), C(4)–C(10)	33.0	28.7
C(1)–C(7), C(9)–C(10)	29.8	25.5
C(1)–C(12), C(10)–C(11)	37.8	34.9
C(2)–C(6), C(4)–C(5)	29.0	23.6
C(5)–C(9), C(6)–C(7)	27.4	23.2
C(7)–C(8), C(8)–C(9)	35.0	30.3
C(2)–CH_3, C(4)–CH_3	43.4	41.1
^{2}J [Hz]:		
C(1)–C(6), C(5)–C(10)	6.4[b])	−5.9
C(2)–C(7), C(4)–C(9)	4.8[b])	−7.0

[a]) Gaussian 03 B3PW91/6-311G**//B3PW91/6-311**. [b]) Sign not determined.

level of theory was chosen for intermediates and transition states with biradical character. All (U)B3PW91 calculations were carried out with the 6-311G(d,p) basis set, using the Gaussian 03 [12] or the Gaussian 98 suite of programs. For all stationary points, frequency calculations were performed; the zero-point vibrational energies were not scaled. In cases in which the $\langle s^2 \rangle$ values were greater than zero, the *Yamaguchi* correction [15] was applied. Intermediates and transition states of the DFT calculations showed substantial biradical character. Therefore, CASSCF calculations were included in this study, which were carried out with the 6-31G(d) basis set (Cartesian, 6d). To assess for dynamic and static electron correlation [16], the energies of the optimized structures were calculated at the CASPT2 level of theory [17]. For these calculations, the program MOLCAS [18] was used.

2.2.2. *Mechanistic Aspects.* The computational investigation of the thermal isomerization of **5b** was carried out in three phases (see *Schemes 1*, *2*, and *4*). First, the barriers of the ring-opening and ring-closure reaction for the transformation shown in *Scheme 1* were determined. The calculations were carried out at the (U)B3PW91/6-311G**//(U)B3PW91/6-311G** level of theory, and by means of the CASPT2(10,10)/6-31G*//CAS(10,10)/6-31G* procedure. The active space for the latter was chosen in a way that the orbitals involved in the formation of **9b** were included as well as those involved in the formation of **7b**. In **5b**, these were the orbitals of the bonds C(2)–C(3), C(3)–C(4), C(7)–C(8), C(6)–C(8), the π bond of C(10)=C(11), and the corresponding antibonding orbitals. For the remaining stationary points, the corresponding orbitals to those of **5b** were used as active space. The results are presented in *Table 2*.

For the reaction depicted in *Scheme 1*, the relative energies (E_{rel}) show that **5b** has to surmount a barrier of 38.5 kcal/mol to form the biradical **10b**, which is a local minimum on the corresponding energy hyper-surface. The internal cyclization of **10b** to the final product **9b** is characterized by a barrier of only 4.2 (B3PW91) or 5.4 kcal/mol (CASPT2(10,10)) in a strongly exothermic process.

The data of *Table 2* further reveal that, at 38.1 (B3PW91) or 38.4 kcal/mol (CASPT2(10,10)), the barrier required to adopt the transition state **TS3** (competitive isomerization of **5b** to oxanorbornatriene **7b**) is slightly lower than the barriers

Scheme 1

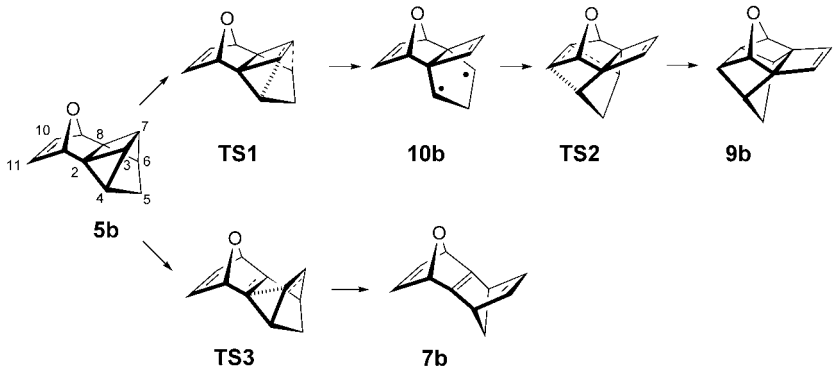

Table 2. *Relative Energies* (E_{rel} [kcal/mol]) *of Selected Stationary Points of the B3PW91/6-311G*** (Method I) *and CASPT2(10,10)/6-31G** (Mehtod II) *Calculations* ($\langle s^2 \rangle$ values of unrestricted DFT calculations)

	E_{rel} (I)[a])[b]) $\langle s^2 \rangle$	E_{rel} (II)
5b	0.00	0.00
TS1	38.47 ⟨0.53735⟩	38.47
10b	34.64 ⟨1.002158⟩	33.58
TS2	38.81 ⟨0.728976⟩	38.96
9b	−27.06	−30.12
TS3	38.12 ⟨1.019181⟩	38.37
7b	−2.00	−7.89
TS4	28.69 ⟨0.461231⟩	29.49
11	26.62 ⟨0.815244⟩	28.40
TS5	30.80 ⟨0.393133⟩	32.30
12	0.70	1.30

[a]) Corrected for zero-point vibrational energies. [b]) Corrected for spin polarization.

separating **5b** from **9b**. In contrast to the **5b** → **9b** conversion, there is no biradical intermediate located between **5b** and oxasesquinorbornatriene **7b**, but **TS3** shows a strong biradical character.

Our computational result indicates that **5b** should isomerize slightly faster to **7b** than to **9b**, which is not compatible with the experimental findings. On this basis, the sole formation of **9a** would require that the model transformation shown in *Scheme 1* were fully reversible and driven thermodynamically to form the most-stable **9a**. Although this cannot be rigorously excluded, the experimental conditions of a flash-vacuum pyrolysis are not favorable for thermodynamic control.

An answer to this problem was obtained by a closer investigation of the energy hyper-surface in the vicinity of the transition state **TS3**. A new thermal reaction path of **5b** was found, which is depicted in *Scheme 2*. In this reaction, the biradical **11** is formed *via* **TS4**. Compound **11** subsequently cyclizes *via* **TS5** to the oxaquadricyclane **12**. The biradical **11** lies energetically only a few kcal/mol below the transition states **TS4** and **TS5**. However, at 30.8 (B3PW91) or 32.3 kcal/mol (CASPT2(10,10)), the barrier

between **5b** and **12** is lower in energy by 6.1–8.1 kcal/mol than the energies of the alternative routes of *Scheme 1*. These data indicate that the thermal isomerization of **5b** will proceed inevitably *via* oxaquadricyclane **12**.

Scheme 2

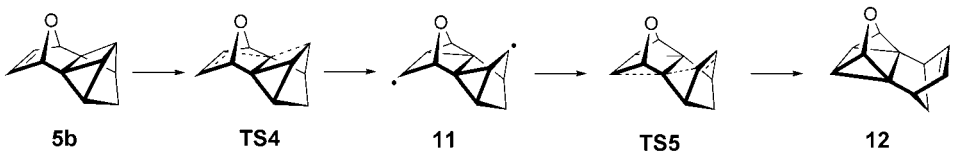

Once arrived at **12**, the further reaction path is easily foreseeable: *Prinzbach* and co-workers have demonstrated in a series of papers that oxaquadricyclanes **13** can open to carbonyl ylides **14** [19], which, in the presence of suitable traps, gave rise to cycloadducts of type **15** [20][21][22] (*Scheme 3*).

Scheme 3

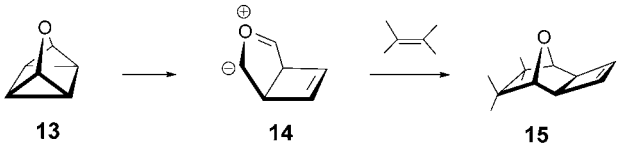

In *Scheme 4*, the reaction sequence from **12** to the cage compound **9b** is shown. The computational results at the (U)B3PW91/6-311G(d,p)//(U)B3PW91/6-311G(d,p) level of theory, of the CAS(8,7)PT2/6-31G(d)//CAS(8,7)/6-31G(d), and of the mp2/6-31G(d)//mp2/6-31G(d) procedure are given in *Table 3*. As, in part, new orbitals are involved in this reaction sequence, a new active space had to be defined for the CAS calculations. The orbitals of **12** responsible for the bonds C(3)–C(4), C(6)–C(7), the π orbital of C(10)=C(11), the corresponding antibonding orbitals, and one of the free electron pairs at the O-atom (the one to become part of the hetero-allyl anion π system in **16**) were chosen.

Scheme 4

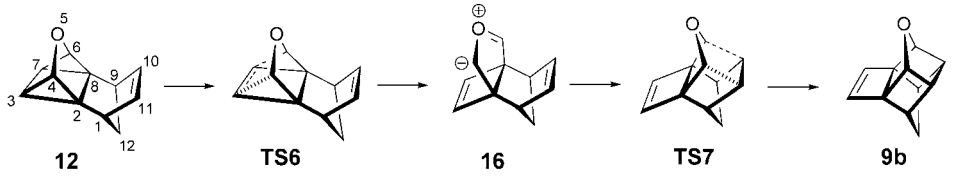

Table 3. *Relative Energies* (E_{rel} [kcal/mol]) *of Selected Stationary Points of the B3PW91/6-311G**** (Method I), *CASPT2(8,7)/6-31G** (Method II), *and mp2/6-311G**** (Method III) *Calculations.* All values were corrected for zero-point vibrational energies.

	E_{rel} (I) $\langle s^2 \rangle$	E_{rel} (II)	E_{rel} (III)
12	0.00	0.00	0.00
TS6	23.08 ⟨0.00⟩	19.23	15.28
16	20.50	11.11	7.89
TS7	23.32 ⟨0.00⟩	14.71	10.98
9b	−27.76	−31.03	−30.15

All three theoretical models indicate that the barriers to the transition states **TS6** and **TS7** are much lower in energy than those leading to **12**. This suggests that **12**, under the reaction conditions, is an intermediate that cannot be isolated and quickly isomerizes to **9b**. Looking somewhat closer at the numbers of *Table 3*, one recognizes that the CAS and the mp2 barriers are significantly lower than the DFT barriers, and the same is true for the 1,3-dipole **16**. However, this inconsistency does not affect the mechanistic interpretation of the formation of **9a** in the thermal isomerization of **5a**, which is supported by all theoretical models used in this investigation.

2.2.3. *Structures of Stationary Points.* The optimized structures of the transition states **TS1**–**TS7** and of the intermediates or products **10b**, **7b**, **11**, **12**, and **16** are depicted in *Fig. 1*, which also shows some selected structural data. At 2.167 Å (*2.146*)[3]), **TS1** shows a strongly elongated C(6)–C(7) distance, indicating a late transition state. The angle C(3)–C(2)–C(4) has widened to 93.26° (*91.37*). In the biradical **10b**, the corresponding angle C(9)–C(1)–C(10) amounts to 117.07° (*116.90*). The five-membered ring C(1)–C(6)–C(7)–C(8)–C(9) is not planar; C(8), H–C(7) and H–C(9) are placed slightly out of the plane C(7)–C(6)–C(1)–C(9) towards the cyclobutene subunit, as indicated for C(8) by the dihedral angle C(1)–C(6)–C(7)–C(8) of 3.73° (*8.60*). This leads to a slight pyramidalization of the radical centers C(7) and C(9). In contrast, **TS2**, which separates the biradical **10b** from **9b**, appears early on the reaction path, as seen by the C(3)–C(9) distance of 2.358 Å (*2.349*). The lengths of the braking bonds of **TS3**, the transition state leading to the oxanorbornatriene **7b**, differ strongly: 2.353 Å (*2.381*) *vs.* 1.768 Å (*1.758*). This asynchronous bond rupture induces a considerable biradical character in **TS3**.

An important structural difference between **TS3** and **TS4** are the distances C(2)–C(11) and C(8)–C(10). In **TS3**, there is no significant shortening of these nonbonding distances with respect to the starting molecule **5b**, which shows a C(2)–C(11) interval of 2.408 Å (*2.431*); the corresponding ones of **TS3** are 2.445 Å (*2.473*) and 2.391 Å (*2.409*). An interesting feature of the structure of oxanorbornatriene **7b** is the pyramidalization of the central C=C bond (dihedral angle C(1)–C(2)–C(7)–C(8) of −169.77° (−*159.56*)). This phenomenon has been detected and studied by several groups for related systems [23] and is not further pursued here.

The transition-state structure **TS4** shows the quadricyclane bond C(7)–C(8) at 1.521 Å (*1.536*) unaffected, and the opposite bond C(2)–C(3) at 2.116 Å (*2.219*) nearly

[3]) Values in italics refer to CAS calculations (see legend to *Fig. 1*).

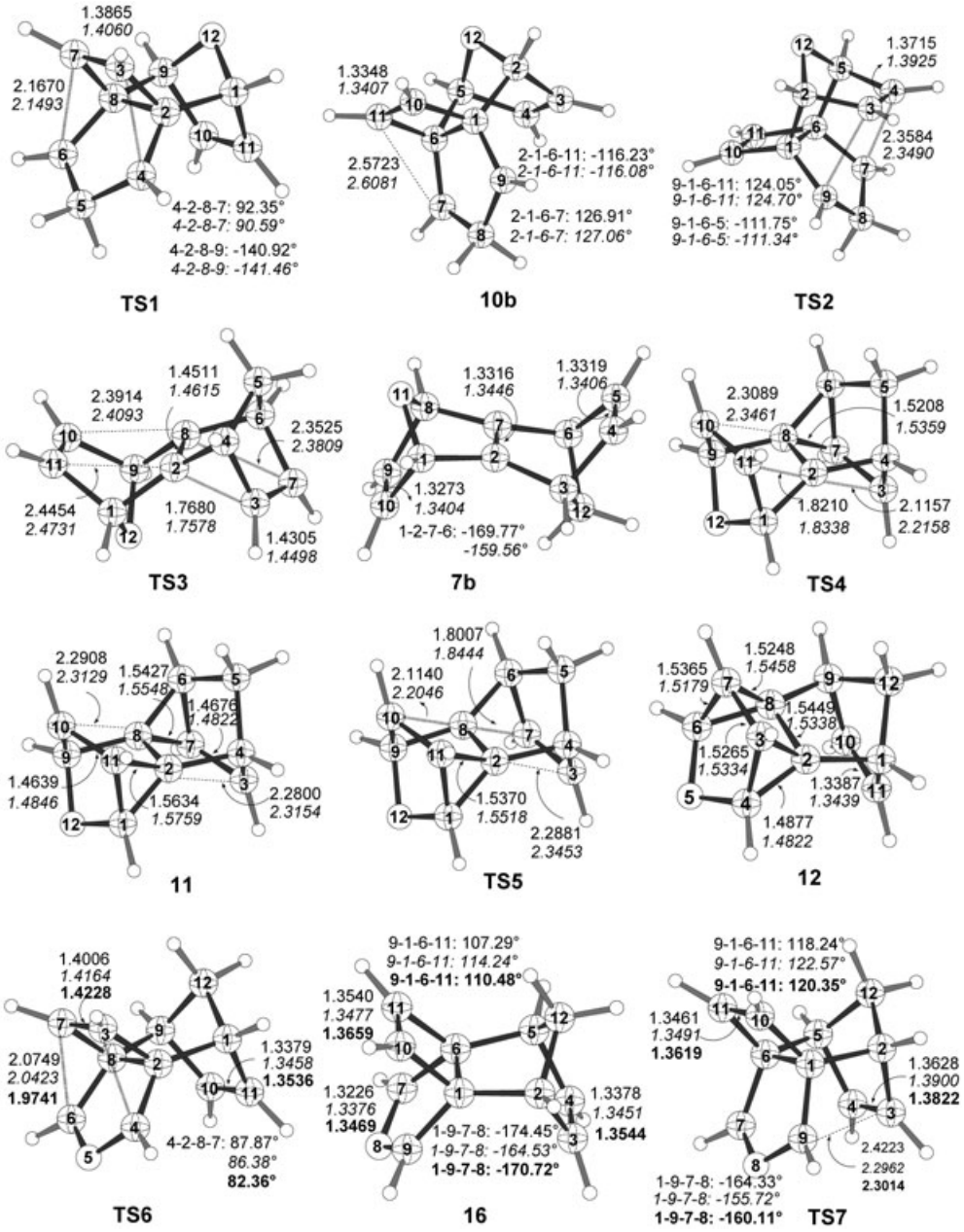

Fig. 1. *Computer-generated structures of the transition states* **TS1**–**TS7**, *and of* **10b**, **7b**, **11**, **12**, *and* **16**. Distances in Å. Regular-type, italicized, and bold values refer to DFT, CAS, and mp2 calculations, resp.

broken, whereas, at 1.821 Å (1.834), the distance between C(2) and C(1) is shortened on its way to become a C–C single bond. In the biradical **11**, the length of the new bond C(2)–C(11) is 1.563 Å (*1.576*), the nonbonded atoms C(8)–C(10) and C(2)–C(3) are at 2.291 Å (*2.313*) and 2.280 Å (*2.315*), respectively. Both radical centers C(3) and C(10) are slightly pyramidalyzed. With respect to biradical **11**, **TS5** shows a shortened C(8)–C(10) distance of 2.114 Å (*2.204*), and a braking C(7)–C(8) bond of 1.801 Å (*1.844*).

An interesting structural feature of the carbonyl ylide **16** is the nonplanarity of the ring made up by C(1)–C(6)–C(7)–O(8)–C(9) (see *Fig. 1*): the O(8)-atom is placed above the plane C(9)–C(1)–C(6)–C(7) towards the four-membered ring. This effect is considerably stronger in the CAS(8,7)/6-31G(d) structure than in the UB3PW91/6-311G(d,p) structure, as indicated by the dihedral angle C(1)–C(9)–C(7)–O(8) of –174.45° (*–164.53*). With respect to the 1,3-dipole **16** as a high-energy intermediate, the transition states **TS6** and **TS7** appear early on the corresponding energy hypersurface. The new bonds to be formed [C(3)–C(4) and C(6)–C(7) in **TS6**, and C(3)–C(9) and C(4)–C(7) in **TS7**] are still very long: 2.075 Å (*2.0431*) in the former, and 2.422 Å (*2.296*) in the latter.

2.3. *Thermal Isomerization of* syn- *and* anti-*Hexacyclo[7.2.1.0^{2,4}.0^{2,8}.0^{3,7}.0^{6,8}]dodec-10-ene*. The unexpected thermal behavior of **5b** to isomerize faster to oxaquadricyclane **12** than to give oxanorbornatriene **7b** prompted us to include the parent hydrocarbons hexacyclo[7.2.1.0^{2,4}.0^{2,8}.0^{3,7}.0^{6,8}]dodec-10-ene, **5c** (*anti*) and **6c** (*syn*), into our computational investigation (*Scheme 5*). In addition to **5c**, **6c**, **7c**, and **8c**, the stationary points **17**, **18**, and **TS8**–**TS11** were calculated at the (U)B3PW91/6-311G(d,p)//(U)B3PW91/6-311G(d,p) and CAS(6,6)Pt2/6-31G(d)//CAS(6,6)6-31G(d) level of theory. The calculations were carried out in detail as indicated above for **5b**. The active space of the CAS(6,6) calculation of **5c** and **6c** consisted of the π orbitals and the braking cyclopropane bonds; the corresponding orbitals of the additional stationary points constituted the active space of these structures. The results of the unrestricted DFT calculations, which showed $\langle s^2 \rangle$ values greater than zero, were corrected for spin polarization, as indicated above. The results are given in *Table 4*.

Table 4 shows for the *anti*-isomer **5c** a substantial energy difference of the barriers **TS9** and **TS8** of 8.4 (UB3PW91) or 9.4 kcal/mol (CASPT2). Under controlled reaction conditions, the degenerate rearrangement of **5c** → **5′c** should be observable at a

Scheme 5

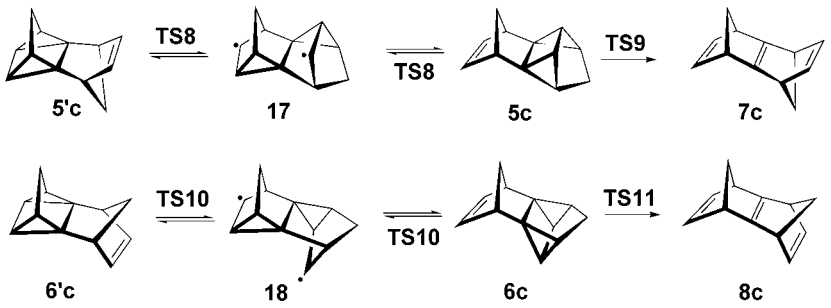

Table 4. *Relative Energies* (E_{rel} [kcal/mol]) *of Different* syn- *and* anti-*Isomers at the (U)B3PW91/6-311G(d,p)//(U)B3PW91/6-311G(d,p)* (Method I) *and CAS(6,6)Pt2/6-31G(d)//CAS(6,6)/6-31G(d)* (Method II) *level*

anti	E_{rel} (I)[a][b])	E_{rel} (II)[a])	*syn*	E_{rel} (I)[a][b])	E_{rel} (II)[a])
5c[c])	0.00	0.00	**6c**[c])	0.00	0.00
TS8	29.01	28.03	**TS10**	41.71	42.21
17	24.99	26.22	**18**	30.74	32.71
TS9	37.39	37.38	**TS11**	35.43	35.62
7c	– 5.72	– 10.70	**8c**	– 10.00	– 15.68

[a]) Corrected for zero-point vibrational energies. [b]) Corrected for spin polarization. [c]) $E(\mathbf{5c}) - E(\mathbf{6c}) =$ – 1.75 kcal/mol for B3PW91 and – 1.57 kcal/mol for CAS(6,6)PT2, resp.

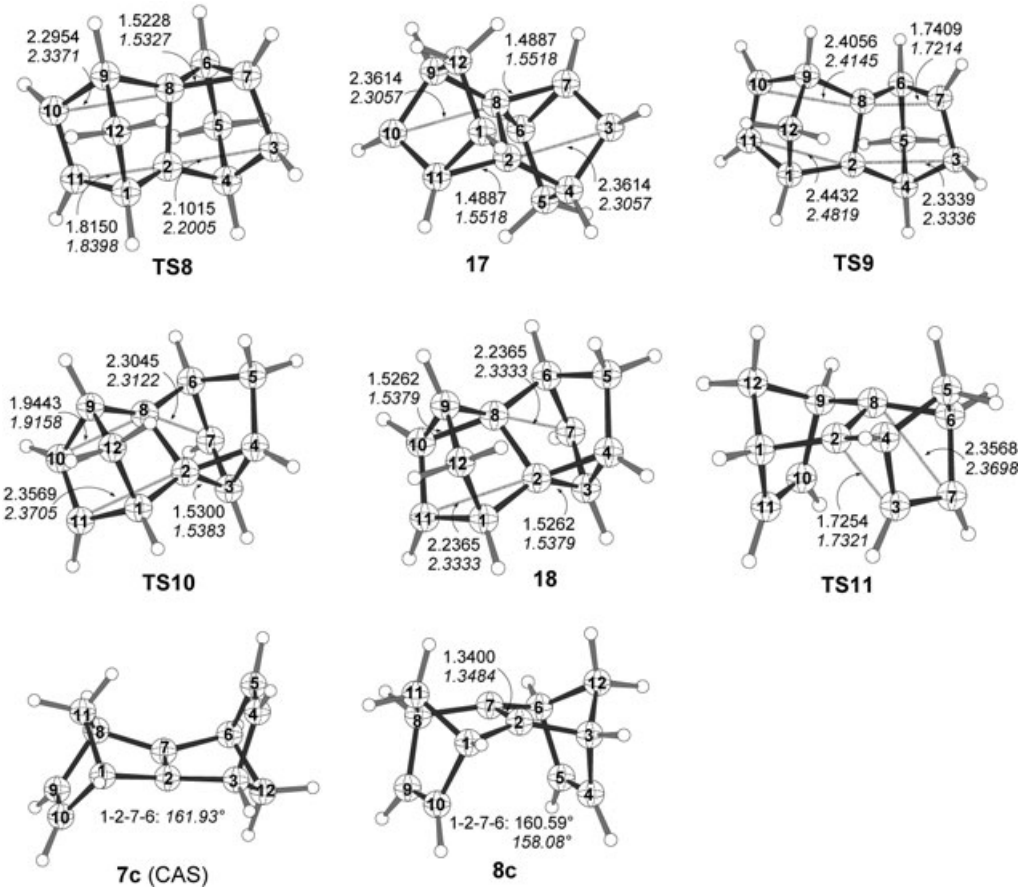

Fig. 2. *Computer-generated structures of selected stationary points* (see *Scheme 5*). Distances in Å. Regular-type and italicized values refer to DFT and CAS calculations, resp.

properly labeled derivative of **5c**. The situation is different for the *syn*-isomer **6c**. Here, **TS10** is higher in energy than **TS11** by 6.3 (UB3PW91) or 6.7 kcal/mol (CASPT2). Compound **6c** will not show the degenerate quadricyclane/quadricyclane reaction, but isomerizes to *syn*-sesquinorbornatriene **8c**. This is in accord with experimental results of *Paquette* and his group [9b].

The structures of some selected stationary points of *Scheme 5* are given in *Fig. 2*, which also shows some important structural details. The interesting features of the pertinent transition states and intermediates are similar to those discussed above for the thermal isomerization of **5b**. Some attention deserves the CAS(6,6)/6-31G(d) structure of **7c** (CAS). The central C(2)=C(7) bond is pyramidalyzed. The planar **7c** (CAS) structure represents a transition state of a degenerate pyramidalization of the

Table 5. *Energies* (*E*; in Hartrees), *Zero-Point Vibrational Energies* (ZPVE; in Hartrees), *Number of Imaginary Frequencies* (NIF), *and* $\langle s^2 \rangle$ *Values for Selected Stationary Points* (see *Schemes 1* and *2*)[a])

	(U)B3PW91/6-311G**//(U)B3PW91/6-311G**	CAS(10,10)Pt2/6-31G*//CAS(10,10)/6-31G*
	E $\langle s^2 \rangle$ ZPVE (NIF) *E*(triplet)[b]) $\langle s^2 \rangle$	*E* ZPVE (NIF)
5b	– 500.1725460	– 498.7043615
	0.180156(0)	0.192666(0)
TS1	– 500.0957718 ⟨0.53735⟩	– 498.6348614
	0.172835(1)	0.184475(1)
	– 500.0734473 ⟨2.010021⟩	
10b	– 500.1115224 ⟨1.002158⟩	– 498.6445073
	0.173602(0)	0.186324(0)
	– 500.1122550 ⟨2.009811⟩	
TS2	– 500.0954512 ⟨0.728976⟩	– 498.6355429
	0.173284(1)	0.185941(1)
	– 500.0807423 ⟨2.008857⟩	
9b	– 500.2176136	– 498.7546941
	0.182100(0)	0.194993(0)
TS3	– 500.1073355 ⟨1.019181⟩	– 498.6391751
	0.176119(1)	0.188619(1)
	– 500.1069169 ⟨2.009331⟩	
7b	– 500.1756523	– 498.7160482
	0.180079(0)	0.191774(0)
TS4	– 500.1135599 ⟨0.461231⟩	– 498.6545166
	0.176319(1)	0.189814(1)
	– 500.0870482 ⟨2.020387⟩	
11	– 500.1199126 ⟨0.815244⟩	– 498.6579696
	0.177313(0)	0.191535(0)
	– 500.1091124 ⟨2.009754⟩	
TS5	– 500.1125359 ⟨0.392476⟩	– 498.653.0053
	0.176308(1)	0.189830(1)
	– 500.0832967 ⟨2.018653⟩	
12	– 500.171553	– 498.7027065
	0.180282(0)	0.193081(0)

[a]) Cartesian coordinates of the stationary points are available on request. [b]) Single-point energy of the triplet of UB3PW91 calculations to account for spin polarization; see [15].

Table 6. *Energies* (*E*; in Hartrees), *Zero-Point Vibrational Energies* (ZPVE; in Hartrees), *Number of Imaginary Frequencies* (NIF), *and* $\langle s^2 \rangle$ *Values for Selected Stationary Points* (see *Scheme 4*)[a])

	(U)B3PW91/6-311G**// (U)B3PW91/6-311G**	CAS(8,7)Pt2/6-31G*// CAS(8,7)/6-31G*	mp2/6-311G**// mp2/6-311G**
	E $\langle s^2 \rangle$ ZPVE (NIF)	*E* ZPVE (NIF)	*E* ZPVE (NIF)
12	– 500.171553	– 498.7028949	– 498.8972729
	0.180282(0)	0.193607(0)	0.180826(0)
TS6	– 500.1311519 ⟨0.00⟩	– 498.6666536	– 498.8686992
	0.176666(1)	0.188013(1)	0.176610(1)
16	– 500.1355098	– 498.6813199	– 498.8816663
	0.176916(0)	0.189734(0)	0.177790(0)
TS7	– 500.1310959 ⟨0.00⟩	– 498.6753793	– 498.8766188
	0.176985(1)	0.189527(1)	0.177677(1)
9b	– 500.2176136	– 498.7542046	– 498.9469799
	0.182100(0)	0.195471(0)	0.182488(0)

[a]) Cartesian coordinates of the stationary points are available from the authors upon request.

C(2)=C(7) bond. However, the barrier vanishes when the zero-point vibrational energy is included in its calculation. In contrast to the CAS result, the B3PW91 structure of **7c** is planar.

Conclusions. – Computational DFT and *ab initio* investigations show that quadricyclanes of the *anti*-hexacyclo[7.2.1.$0^{2,4}$.$0^{2,8}$.$0^{3,7}$.$0^{6,8}$]dodec-10-ene type (**5b** and **5c**) isomerize thermally *via* biradicals **11** and **17** to the quadricyclanes **12** or **5′c**, respectively. Oxaquadricyclane **12** undergoes an experimentally well-established cycloreversion to the carbonyl ylide **16**, which reacts in a 1,3-dipolar addition to the internal C=C bond to form the bishomocubane derivative **9b**. The lowest energy barrier for the thermal reaction of *syn*-hexacyclo[7.2.1.$0^{2,4}$.$0^{2,8}$.$0^{3,7}$.$0^{6,8}$]dodec-10-ene (**6c**) is the conversion to the *syn*-sesquinorbornatriene **8c**.

We thank Dr. *D. Stephenson*, Universität München, for the NMR measurements, and Dr. *P. Wessig*, Humboldt-Universität Berlin, for his help with the MOLCAS program.

Experimental Part

Thermal Isomerization of **5a**. A *ca.* 3:1 mixture (300 mg, 1.61 mmol) of *anti*- (**5a**) and *syn*-1,9-dimethyl-12-oxahexacyclo[7.2.1.$0^{2,4}$.$0^{2,8}$.$0^{3,7}$.$0^{6,8}$]dodec-10-ene (**6a**), obtained as reported earlier [2], was distilled at 0.001 Torr through a glass spiral (length 25 cm), which was placed in a tube oven (*Heraeus RO 4/25*) at 350°. The volatile material was condensed in a dry-ice/acetone-cooled trap. *2,4-Dimethyl-3-oxahexacyclo[5.5.0.0^{1,10}.0^{2,6}.0^{4,10}.0^{5,9}]-dodec-11-ene* (**9a**; 250 mg, 83%) was isolated as the sole product, besides some minor impurities (NMR) of unknown structure.

Data of **9a**. Colorless oil. UV ($CHCl_3$): λ_{max} (log ε) 321 (3.04), 396 nm (2.63). IR (film): 3356, 2972, 2929, 2865, 1681, 1448, 1376, 1286, 1103, 906, 790, 731 cm^{-1}. ^{1}H-NMR (400 MHz, $CDCl_3$)[4]): δ 1.52 (*s*, 2 Me); 1.98 (*dt*, ^2J = 11.8 Hz, ^3J = 1.5 Hz, 1 H of CH_2(8)); 2.16 (*dt*, ^2J = 11.8 Hz, 1 H of CH_2(8)); 2.56 (*m*, 2 H, H–C(7),

[4]) The structure of **9a** was established by INADEQUATE NMR experiments. The ^{13}C,^{13}C-NMR coupling constants are given in *Table 1*.

Table 7. *Energies* (*E*; in Hartrees), *Zero-Point Vibrational Energies* (ZPVE; in Hartrees), *Number of Imaginary Frequencies* (NIF), *and* $\langle s^2 \rangle$ *Values for Selected Stationary Points* (see *Scheme 5*)[a])

	(U)B3PW91/6-311G(d,p)// (U)B3PW91/6-311G(d,p) *E* $\langle s^2 \rangle$ ZPVE (NIF) *E*(triplet)[b]) $\langle s^2 \rangle$	CAS(6,6)Pt2/6-31G(d)// CAS/6,6)/6-31G(d) *E* ZPVE (NIF)
5c	– 464.2890225 0.204298(0)	– 462.8586427 0.218993(0)
TS8	– 464.2317109 ⟨0.423578⟩ 0.200545(1) – 464.2041025 ⟨2.019772⟩	– 462.8109872 0.216013(1)
17	– 464.2396001 ⟨0.835961⟩ 0.201469(0) – 464.2300955 ⟨2.00976⟩	– 462.8156857 0.217813(0)
TS9	– 464.224049 ⟨0.983874⟩ 0.200050(1) – 464.2228583 ⟨2.010305⟩	– 462.7950314 0.214945(1)
7c	– 464.2982407 0.204405(0)	– 462.8747730[b]) 0.218068(0) – 462.8743261[b]) 0.217686(1)
6c	– 464.2860758 0.204146(0) –	– 462.8560500 0.218897(0)
TS10	– 464.2161120 ⟨1.027242⟩ 0.199900(1) – 464.2168569 ⟨2.037691⟩	– 462.7853360 0.215455(1)
18	– 464.2338452 ⟨1.004950⟩ 0.201063(0) – 464.2336874 ⟨2.00992⟩	– 462.8028274 0.217798(0)
TS11	– 464.2258815 ⟨1.010826⟩ 0.200332(1) – 464.225964 ⟨2.009043⟩	– 462.7953098 0.214929(1)
8c	– 464.3027079 0.204850(0)	– 462.8805453 0.218403(0)

[a]) Cartesian coordinates of the stationary points are available from the authors upon request. [b]) Single-point energy of the triplet of UB3PW91 calculations to account for spin polarization; see [15].

H–C(9)); 2.65 (*m*, H–C(5), H–C(6)); 6.17 (*s*, H–C(11), H–C(12)). ^{13}C-NMR (101 MHz, $CDCl_3$): δ 14.50 (Me); 40.54 (C(7), C(9)); 40.82 (C(8)); 52.48 (C(5), C(6)); 71.04 (C(1), C(10)); 88.61 (C(2), C(4)); 138.20 (C(11), C(12)). EI-MS (70 eV): *m*/*z* 186 (4, M^+), 171 (6), 146 (6), 144 (6), 92 (77), 74 (11), 57 (100). HR-MS: 186.1162 (M^+, $C_{13}H_{14}O^+$; calc. 186.1045). Results of the MO calculations are summarized in *Tables 5–7*.

REFERENCES

[1] O. Baumgärtel, G. Szeimies, *Chem. Ber.* **1983**, *116*, 2180; O. Baumgärtel, J. Harnisch, G. Szeimies, M. Van Meerssche, G. Germain, J.-P. Declercq, *Chem. Ber.* **1983**, *116*, 2205.
[2] J. Kenndoff, K. Polborn, G. Szeimies, *J. Am. Chem. Soc.* **1990**, *112*, 6117.
[3] J. Podlech, K. Polborn, G. Szeimies, *J. Org. Chem.* **1993**, *58*, 4113.
[4] U. Heywang, G. Szeimies, *Chem. Ber.* **1990**, *123*, 121.

[5] J. Podlech, Dissertation, Universität München, 1993.
[6] G. Szeimies, *J. Prakt.Chem.* **1998**, *340*, 11.
[7] L. A. Paquette, H. Künzer, K. E. Green, O. De Lucchi, G. Licini, L. Pasquato, G. Valle, *J. Am. Chem. Soc.* **1986**, *108*, 3453.
[8] L. A. Paquette, H. Künzer, *J. Am. Chem. Soc.* **1986**, *108*, 7431.
[9] a) H. Künzer, E. Litterst, R. Gleiter, L. A. Paquette, *J. Org. Chem.* **1987**, *52*, 4744; b) L. A. Paquette, H. Künzer, M. A. Kesselmayer, *J. Am. Chem. Soc.* **1988**, *110*, 6521.
[10] P. Camps, J. A. Fernández, S. Vázquez, M. Font-Bardia, X. Solans, *Angew. Chem., Int. Ed.* **2003**, *42*, 4049.
[11] A. E. Derome, 'Modern NMR Techniques for Chemistry Research', Pergamon Press, Oxford, 1987, p. 234 – 239.
[12] Gaussian 03, Revision C.02, M. J. Frisch, G. W. Trucks, H. B. Schlegel, G. E. Scuseria, M. A. Robb, J. R. Cheeseman, J. A. Montgomery Jr., T. Vreven, K. N. Kudin, J. C. Burant, J. M. Millam, S. S. Iyengar, J. Tomasi, V. Barone, B. Mennucci, M. Cossi, G. Scalmani, N. Rega, G. A. Petersson, H. Nakatsuji, M. Hada, M. Ehara, K. Toyota, R. Fukuda, J. Hasegawa, M. Ishida, T. Nakajima, Y. Honda, O. Kitao, H. Nakai, M. Klene, X. Li, J. E. Knox, H. P. Hratchian, J. B. Cross, V. Bakken, C. Adamo, J. Jaramillo, R. Gomperts, R. E. Stratmann, O. Yazyev, A. J. Austin, R. Cammi, C. Pomelli, J. W. Ochterski, P. Y. Ayala, K. Morokuma, G. A. Voth, P. Salvador, J. J. Dannenberg, V. G. Zakrzewski, S. Dapprich, A. D. Daniels, M. C. Strain, O. Farkas, D. K. Malick, A. D. Rabuck, K. Raghavachari, J. B. Foresman, J. V. Ortiz, Q. Cui, A. G. Baboul, S. Clifford, J. Cioslowski, B. B. Stefanov, G. Liu, A. Liashenko, P. Piskorz, I. Komaromi, R. L. Martin, D. J. Fox, T. Keith, M. A. Al-Laham, C. Y. Peng, A. Nanayakkara, M. Challacombe, P. M. W. Gill, B. Johnson, W. Chen, M. W. Wong, C. Gonzalez, J. A. Pople, *Gaussian, Inc.*, Wallingford CT, 2004.
[13] A. D. Becke, *J. Chem. Phys.* **1993**, *98*, 5648.
[14] J. P. Perdue, K. Burke, Y. Wang, *Phys. Rev. B.* **1996**, *54*, 16533, and refs. cit. therein.
[15] K. Yamaguchi, F. Jensen, A. Dorigo, K. N. Houk, *Chem. Phys. Lett.* **1988**, *149*, 537.
[16] W. T. Borden, E. R. Davidson, *Acc. Chem. Res.* **1996**, *29*, 67.
[17] K. Andersson, P.-A. Malmqvist, B. O. Roos, A. J. Sadlej, K. Wolinski, *J. Phys. Chem.* **1990**, *94*, 5483; K. Andersson, P.-A. Malmqvist, B. O. Roos, *J. Phys. Chem.* **1992**, *96*, 1218.
[18] K. Andersson, M. Barysz, A. Bernhardsson, M. R. A. Blomberg, D. L. Cooper, T. Fleig, M. P. Fülscher, C. de Graf, B. A. Hess, G. Karlström, R. Lindh, P.-Å. Malmquist, P. Neogrády, J. Olsen, B. O. Ross, A. J. Sadlej, M. Schütz, B. Schimmelpfennig, L. Seijo, L. Serrano-Andrés, P. E. M. Siegbahn, J. Stålring, T. Thorsteinsson, V. Veryazov, P.-O. Widmark, MOLCAS, Version 5.2, Lund University, Sweden, 2001.
[19] V. Markowski, R. Huisgen, *J. Chem. Soc., Chem. Commun.* **1977**, 439; R. Huisgen, V. Markowski, *J. Chem. Soc., Chem. Commun.* **1977**, 440, and refs. cit. therein.
[20] H. Prinzbach, H. Babsch, *Angew. Chem., Int. Ed.* **1975**, *14,* 753; H. Prinzbach, H. Bingmann, J. Markert, G. Fischer, L. Knothe, W. Eberbach, J. Brokatzky-Geiger, *Chem. Ber.* **1986**, *119*, 589, and refs. cit. therein.
[21] W. Tochtermann, G. Olsson, *Chem. Rev.* **1989**, *89*, 1203.
[22] E. Hasselbach, H.-D. Martin, *Helv. Chim. Acta* **1974**, *57*, 472.
[23] R. V. Williams, D. Margetić, *J. Org. Chem.* **2004**, *69*, 7134; D. Margetić, R. V. Williams, R. N. Warrener, *J. Org. Chem.* **2003**, *68*, 9186, and refs. cit. therein.

Received February 25,2005